Available online at www.sciencedirect.com
ScienceDirect
Journal of Hazardous Materials 145 (2007) 437–452
Journal of Hazardous Materials
www.elsevier.com/locate/jhazmat

# Development and validation of a model of bio-barriers for remediation of Cr(VI) contaminated aquifers using laboratory column experiments

T. Shashidhar, S. Murty Bhallamudi, Ligy Philip *

*Department of Civil Engineering, Indian Institute of Technology Madras, Chennai 600036, Tamilnadu, India*

Received 20 March 2006; received in revised form 16 November 2006; accepted 16 November 2006
Available online 21 November 2006

**Abstract**

Bench scale transport and biotransformation experiments and mathematical model simulations were carried out to study the effectiveness of bio-barriers for the containment of hexavalent chromium in contaminated confined aquifers. Experimental results showed that a 10 cm thick bio-barrier with an initial biomass concentration of 0.205 mg/g of soil was able to completely contain a Cr(VI) plume of 25 mg/L concentration. It was also observed that pore water velocity and initial biomass concentration are the most significant parameters in the containment of Cr(VI). The mathematical model developed is based on one-dimensional advection-dispersion reaction equations for Cr(VI) and molasses in saturated, homogeneous porous medium. The transport of Cr(VI) and molasses is coupled with adsorption and Monod's inhibition kinetics for immobile bacteria. It was found that, in general, the model was able to simulate the experimental results satisfactorily. However, there was disparity between the numerically simulated and experimental breakthrough curves for Cr(VI) and molasses in cases where there was high clay content and high microbial activity. The mathematical model could contribute towards improved designs of future bio-barriers for the remediation of Cr(VI) contaminated aquifers.


*Keywords:* Bio-barrier; Biotransformation; Hexavalent chromium; Column experiments; Contaminant transport model

## 1. Introduction

As reported from several parts of the world, both anthropogenic and natural processes may lead to hexavalent chromium contamination in soils and aquifers. Industrial activities such as electroplating, leather tanning, and wood preservation, etc. release large quantities of liquid and solid waste containing Cr(VI) [1]. Hexavalent Chromium is highly toxic, highly soluble in water, and is likely to be transported over long distances in the subsurface. Two alternatives are available for treating the Cr(VI) contaminated groundwater: (i) pump and treat, and (ii) in situ. These can be achieved either by physico-chemical or biological processes. Latter method appears to be more economical and environmentally friendly. Several researchers have reported that many micro-organisms, under various environmental conditions, can reduce highly toxic and mobile Cr(VI) to less toxic and less mobile Cr(III) [2–4].

Studies have been conducted in the past to evaluate the potential of biotransformation for the remediation of Cr(VI) contaminated soil and wastewater. Most of these studies pertain to ex situ treatment option [5–7]. Experiments have also been conducted to understand the combined transport and geo-chemical processes pertaining to Cr(VI) in different soils through batch and continuous column studies [8–12]. Several batch studies on biotransformation of Cr(VI) to Cr(III) under various environmental conditions [13–15] have been reported. Recently, combined transport and biotransformation studies have been reported by Guha [16] and Shashidhar et al. [17]. Guha [16] focused on the transport of Cr(VI) through saturated column with manganese coated sand, under the influence of adsorption, competitive redox and biotransformation. However, he used small laboratory scale columns (10–30 cm long) for this purpose. Experimental data was available only for the inlet and outlet, which may not be sufficient to completely understand the interplay between geo-hydrology and chromium containment. Shashidhar et al. [17] conducted bench-scale column experiments to evaluate the effectiveness of Cr(VI) containment in aquifers using bioremediation. Effects of ground water velocity,

* Corresponding author. Tel.: +91 44 2257 4274; fax: +91 44 2257 4252.
*E-mail address:* ligy@iitm.ac.in (L. Philip).

0304-3894/$ – see front matter © 2006 Elsevier B.V. All rights reserved.
doi:10.1016/j.jhazmat.2006.11.034

initial microbial concentration, and aquifer soil characteristics on Cr(VI) containment were studied. Experiments were also conducted to study only the transport and adsorption of Cr(VI) in order to assess the role of bioremediation in Cr(VI) containment. Although there have been many studies which considered the effectiveness of Cr(VI) containment in confined aquifers using bio-barriers, not many studies on validation of mathematical models for such systems using systematic laboratory experimental data are reported.

The objective of the present study was to conduct, in continuation of authors' earlier study [17], further bench-scale column studies for evaluating the performance of bio-barriers for the remediation of Cr(VI) contaminated confined aquifers. Also, an attempt was made to develop and validate a mathematical model for predicting the containment of Cr(VI) in contaminated confined aquifers by in situ bioremediation.

## 2. Materials and methods

### 2.1. Soil

Soils used in this study were collected from the I.I.T. Madras campus, Chennai, India. The portion which passed through 4.75 mm sieve opening was used for the experiment. River sand which passed through 0.6 mm and retained in 0.425 mm sieve opening was washed thoroughly with distilled water and oven dried at 103 °C over night before being used in sand column experiments. The soil and sand characteristics were analyzed as per the standard methods [18] and are presented in Table 1.

### 2.2. Chemicals

All the chemicals used in this study were of AR grade and were supplied by Ranbaxy Chemicals Ltd., Chennai, India. Glassware used for analysis were equilibrated with Cr(VI) and washed with acid solution followed by distilled water.

Table 1
Soil characteristics

| S. No. | Properties | Value | | |
|---|---|---|---|---|
| | | Soil C | Sand | Soil A |
| 1 | Clay content (%) | 3.1 | 0 | 6.19 |
| 2 | Silt content (%) | 11.35 | 0 | 22.70 |
| 3 | Sand content (%) | 85.55 | 100 | 71.11 |
| 4 | Specific gravity | 2.6 | 2.63 | 2.543 |
| 5 | Organic content (%) | 0.1 | 0 | 0.92 |
| 6 | Bulk density (g/cm$^3$) | 1.6 | 1.41 | 1.6 |
| 7 | Porosity | 0.37 | 0.45 | 0.375 |
| 8 | Iron content (mg/g) | 1.008 | 0.771 | 0.890 |
| 9 | Manganese content (mg/g) | 0.106 | 0.053 | 0.080 |

### 2.3. Nutrient medium

The medium (M2) for Cr(VI) reduction experiments consisted of $K_2HPO_4$ (0.03 g/L), $KH_2PO_4$ (0.05 g/L), $MgSO_4{\cdot}7H_2O$ (0.01 g/L), $NH_4Cl$ (0.03 g/L), NaCl (0.01 g/L), carbon source (2 g/L), and 1 mL of trace element solution. The carbon source used in the present study was molasses (measured as COD), which was prepared synthetically from crude sugar, known as "jaggery". Trace element solution consisted of $FeCl_2{\cdot}4H_2O$ (12.2 g/L), $MnCl_2{\cdot}4H_2O$ (4.09 g/L), $CoCl_2{\cdot}6H_2O$ (0.927 g/L), $ZnCl_2$ (0.37 g/L), $CuCl_2$ (0.61 g/L), $NaMoO_4{\cdot}2H_2O$ (0.579 g/L), $H_3BO_3$ (0.16 g/L), KI (0.148 g/L), $NiCl{\cdot}6H_2O$ (0.067 g/L), and EDTA $Na_2{\cdot}4H_2O$ (6.5 g/L). The pH was maintained at $7 \pm 0.2$ by using HCl or NaOH. Molasses was used as a carbon source. Sterilized medium was used for all the studies.

### 2.4. Enrichment of Cr(VI) reducing bacterial strains

Bacterial strains were isolated from the soil samples collected from the chromium contaminated site located at Ranipet,

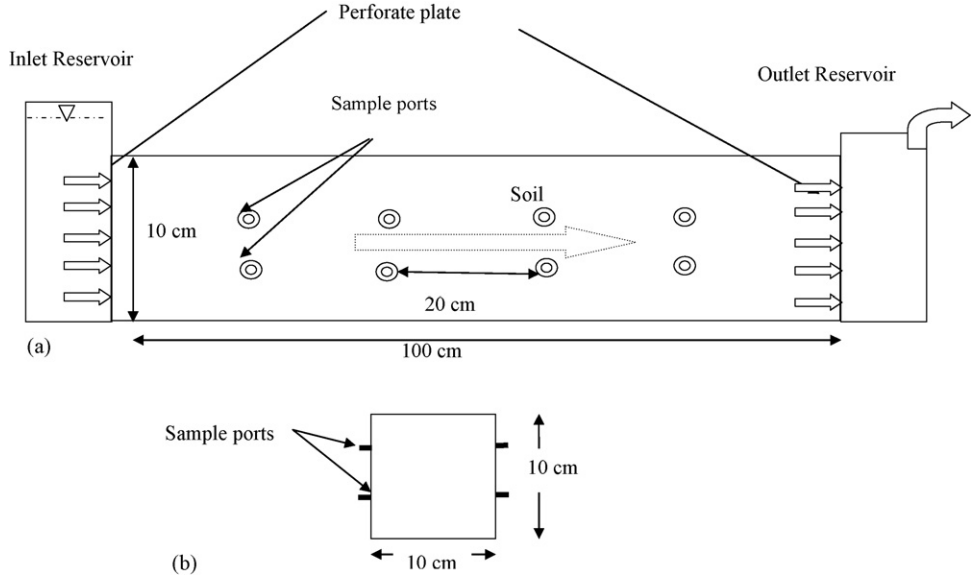


Fig. 1. Schematic of experimental setup.

Tamilnadu, India. Detailed methodology for the enrichment, cultivation and harvesting of Cr(VI) reducing bacterial strains is presented elsewhere [6,17].

### 2.5. Experimental setup

Fig. 1a shows the schematic of the bench scale experimental setup used in this study. The length of the column was 1 m and it had a 10 $cm^2$ cross section, with an effective radius of 10 cm. This was fabricated in the laboratory using PVC (Perspex) sheets of 6 mm thickness. The column was filled with thoroughly washed pure river sand from 0 to 50 cm, and again from 60 to 100 cm. To simulate the bio-barrier conditions, the portion between 50 and 60 cm was filled with Soil-A augmented with Cr(VI) reducing microbes. An overhead tank with provision for an adjustable head served as the inlet to the column. A uniform entry of water into the soil was ensured by providing a porous plate at the inlet. The effluent was collected in a tank provided at the outlet. Saturated conditions in the column were achieved by maintaining the water level in the outlet reservoir above the top of the soil column. Sampling ports were provided on the sides at five different cross sections at distances 20, 40, 49, 60, and 80 cm from the inlet, respectively. As shown in Fig. 1b, four ports were provided at each cross-section. Sterilized disposal syringes (Dispovan, India) were used to collect liquid samples from these ports at regular time intervals.

### 2.6. Batch studies

Sorption equilibrium studies for Cr(VI), alone and in presence of molasses and lithium were conducted using Soils A, C, and sand, to estimate the adsorption coefficients. The details of these studies are presented elsewhere [17]. Similarly, biokinetic studies were conducted as per standard procedure to estimate the kinetic parameters of Cr(VI) reducing microbial consortia [19].

### 2.7. Transport and biotransformation studies

#### 2.7.1. Transport studies without biotransformation

The column was filled with prepared soil in 33 layers. In order to get a more or less uniform compaction, each layer was compacted with 25 blows of a 1.2 kg hammer falling from a 30 cm height. Bulk density was determined by measuring the dry weight of the soil before adding the required moisture and filling the column. The porosity was determined using the formula relating the bulk density, and dry weight. Initially, steady flow rate through the soil column was obtained by maintaining constant heads in the head and tail tanks for a long time. The flow rate was monitored with respect to time by collecting the water at the outlet. Cr(VI) contaminated water was introduced into the system through the head tank after the steady state was attained. Liquid samples were taken from all the sampling ports as well as the head tank at regular time intervals, and were analyzed for Cr(VI) concentration. Experiment was continued until the breakthrough occurred at the last sampling cross section. These experiments were conducted for Soil-A with a porosity of 0.375, for three different velocities of 22.4, 11.2, and 5.6 cm/h, respectively.

Table 2
Transport and biotransformation studies

| Soil type | Initial pore velocity (cm/h) | Bacterial conc. added (mg/g) | Column length (cm) |
|---|---|---|---|
| Soil C | 7.32 | 0.0232 | 100 |
| Sand | 6.67 | 0.0205 | 100 |
| Sand | 1.16 | 0.0405 | 100 |
| Soil A | 5.833 | 0.0205 | 100 |
| Bio-barrier study | | | |
| Soil A | 1.98 | 0.0205 | 10[a] |
| Soil A | 2.66 | 0.205 | 10[a] |

[a] Bio-barrier thickness (cm).

#### 2.7.2. Transport studies with biotransformation

Transport studies with biotransformation were conducted in a similar manner. However, in these tests, the soil was mixed with bacterial cells and mineral medium. The column was fed with mineral medium until a steady state velocity was attained. The column was then fed with medium containing 25 mg/L of Cr(VI), molasses (approximately 2000 mg/L of COD), and lithium (50 mg/L) along with minerals. Samples were withdrawn from various sampling ports at regular intervals using syringes and were analyzed. Other details of the procedure are given elsewhere [17]. These studies were conducted with two different soils namely Soils A, and C and with sand as given in Table 1.

#### 2.7.3. Transport studies with bio-barriers

Transport studies with bio-barriers were conducted in a similar manner to those without bio-barriers, except that a bio-barrier of 10 cm thickness was provided at a distance of 50 cm from the inlet. The 10 cm bio-barrier was filled with Soil A, mixed with microbes, whereas the rest of the column was filled with sand without any microbes. Also, four more sampling ports were provided at 49 cm from the inlet, i.e. just at the starting of the bio-barrier. Two vents were provided for release of gasses generated in the bio-barrier. As in the column studies without bio-barriers, concentrations of microbes, substrate Cr(VI), and lithium in liquid phase were monitored continuously at all the ports. Flow rate and microbial concentration were also monitored at the outlet. After the completion of column run, soil samples were taken from different ports and were analyzed for adsorbed Cr(VI), total chromium, COD, lithium, and microbial concentration. These column studies with bio-barriers were conducted for two different initial microbial concentrations in the barrier. The experimental details for all the transport studies with biotransformation are presented in Table 2.

### 2.8. Analytical procedures

#### 2.8.1. Liquid phase chromium analysis

Diphenyl carbazide method was used to determine the Cr(VI) concentration [20]. Total chromium concentration was analyzed using atomic absorption spectrometer (Perkin Elmer, USA).

*2.8.2. Extraction and analysis of Cr(VI) and total chromium in soil*

Alkaline digestion method and nitric acid/sulfuric acid digestion method as per Standard Methods were used for the extraction of Cr(VI) and total chromium from soil, respectively. Diphenyl carbazide method was used to determine the Cr(VI) concentration [20]. Potassium permanganate was used to oxidize Cr(III) to Cr(VI) in the case of Cr(III).

*2.8.3. Measurement of cell density in liquid phase*

Cells were grown overnight, centrifuged, washed with physiological saline water thrice, re-suspended in saline water, homogenized, and used as stock solution. Different dilutions were made from the above stock solution. Dry weights of cells were measured by filtering a known volume of these solutions through 0.45 μm filter paper (Millipore, USA). Corresponding absorbance was measured at 440 nm using a spectrophotometer. This information was used to prepare a calibration curve between dry weight and absorbance. For unknown samples, the absorbance was measured at 440 nm and was converted to dry weight using absorbance versus dry weight calibration curve.

*2.8.4. Microbial quantification*

The bacterial cell count (colony forming units) was carried out as per standard procedure [20]. The total protein of intact cells was determined according to the method of Herbert et al. [21]. The cell suspension (0.5 mL) was mixed with 2 mL of 1.0 N NaOH and was kept in boiling water bath for 5 min. The contents were then cooled in cold water. To this, 5 mL of freshly prepared alkaline copper reagent was added and allowed to stand for 10 min. 0.5 mL of Folin-Ciocalteu reagent was then added and allowed to stand for 30 min for the color development. Reagent blank containing 0.5 mL distilled water instead of bacterial suspension was treated in a similar way. The optical density was measured at 750 nm using a spectrometer against the reagent blank. Known bacterial concentrations were used for preparing the calibration curve.

*2.8.5. Chemical oxygen demand*

COD of liquid and soil samples were estimated as per standard methods [20]. Closed reflex method was followed.

*2.8.6. Lithium*

Lithium was analyzed using flame photometer (Elico, India) method as described in standard methods [20].

## 3. Mathematical model

Mathematical model for the transport accounts for the advective-dispersive-reactive transport of three aqueous species: Li, Cr(VI), and substrate (molasses). Lithium, a conservative pollutant, was used as a tracer. Therefore, Li transport data was used to determine the dispersion coefficient. The column experiments showed that Cr(III) formed due to biotransformation of Cr(VI) did not remain in the liquid phase and it was either precipitated and retained or adsorbed onto the soil matrix almost immediately. Liquid samples, collected from all the 16 ports and the outlet tank, did not contain any Cr(III). Therefore, Cr(III) transport is not included in the present mathematical model.

In the column experiments, there was washout of microbes during the initial stabilization. During this period, water with only mineral medium was allowed to pass through the column until steady state flow conditions were achieved. The amount of washout depended upon the soil. There were more washouts of microbes in columns with sand as compared to those in columns with soil. It may be noted that although there was washout during the stabilization period, the liquid samples taken from 16 ports as well as the outlet tank did not contain significant amount of microbes once the stabilization was achieved. Therefore, it was assumed that the microbes were immobile and attached to the soil matrix. Only the microbial growth equation was considered and the transport of microbes in the liquid phase was neglected.

It may be noted that in an earlier study on bio-geochemical transport of Cr(VI) through sand columns, Guha [16] used a similar approach to modeling the transport and transformation of Cr(VI). However, in that model, it was assumed that some bacteria were mobile and some were immobile. Also, a double Monod's kinetic equation was used for microbial growth, in which both Lactate (electron donor) and Cr(VI) (electron acceptor) were treated as substrate. In this study, the Monod's equation with inhibition was used to model the microbial growth. Batch studies indicated that molasses (substrate) concentration was not limiting, while Cr(VI) concentration used was much above the inhibition concentration (3.05 mg/L). Also, the batch studies indicated that not all the molasses present was available for microbial utilization. In the present study, the carbon source used (referred to as molasses) was crude sugar, known as 'jaggery'. It contains a mixture of sucrose, cellulose, etc. In this, sucrose is the only easily biodegradable substrate available. After the complete utilization of sucrose, the microbes start utilizing cellulose slowly, as it is not an easily biodegradable substrate. In the present study, the time available was limited for degradation of cellulose. Therefore, the concept of utilizable substrate [22] was adapted in the model for microbial growth rate. Another modification made to the usual microbial growth rate equation was the introduction of a parameter, λ which is similar to the microbial metabolic potential factor used by other researchers [16,23].

The governing advection-dispersion reaction equations for one-dimensional transport of lithium, hexavalent chromium, substrate, and microbes can be written as follows:

$$\frac{\partial \mathrm{Li}}{\partial t} + u\frac{\partial \mathrm{Li}}{\partial x} = D\frac{\partial^2 \mathrm{Li}}{\partial x^2} \tag{1}$$

$$R_{\mathrm{Cr6}}\frac{\partial \mathrm{Cr6}}{\partial t} + u\frac{\partial \mathrm{Cr6}}{\partial x} = D\frac{\partial^2 \mathrm{Cr6}}{\partial x^2} - R_{\mathrm{sinkCr6}} \tag{2}$$

$$R_{\mathrm{s}}\frac{\partial S}{\partial t} + u\frac{\partial S}{\partial x} = D\frac{\partial^2 S}{\partial x^2} - R_{\mathrm{sinkS}} \tag{3}$$

$$R_{\mathrm{sinkS}} = \frac{\mathrm{d}S}{\mathrm{d}t} \tag{4}$$

$$\frac{\mathrm{d}S}{\mathrm{d}t} = \frac{\lambda\mu M}{Y} \tag{5}$$

$$\mu = \left(\frac{\mu_{\max} \mathrm{Su}}{K_s + \mathrm{Su}}\right)\left(\frac{K_i}{K_i + \mathrm{Cr6}}\right) \quad (6.a)$$

$$\mu = 0, \quad \text{if } \mathrm{Su} < 0 \quad (6.b)$$

$$\mathrm{Su} = S - 0.63 S_T \quad (7)$$

$$\frac{1}{M}\left(\frac{dM}{dt}\right) = \lambda(\mu - k_d) \quad (8)$$

$$R_{\mathrm{sinkCr6}} = \frac{M\lambda\eta\mu}{Y} \quad (9)$$

where Li is the lithium concentration in the liquid medium (mg/L), Cr6 the hexavalent chromium concentration in the liquid medium (mg/L), $S$ the molasses concentration in the liquid medium (mg/L), $M$ the bacterial concentration expressed as mg/L of liquid in the column, Su the utilizable concentration of molasses (mg/L), $S_T$ the total inlet molasses concentration (mg/L), $u$ the pore water velocity (cm/h), $D$ the coefficient of dispersion ($cm^2$/h), $R_{Cr6}$ the retardation coefficient for hexavalent chromium, $R_s$ the retardation coefficient for substrate, $R_{\mathrm{sink\ Cr6}}$ the sink term for hexavalent chromium due to biotransformation (mg/L/h), $R_{\mathrm{sink\ S}}$ the sink term for substrate due to microbial utilization (mg/L/h), $\mu$ the specific growth rate ($h^{-1}$), $\mu_{\max}$ the maximum specific growth rate ($h^{-1}$), $k_d$ the decay constant ($h^{-1}$), $Y$ the observed yield coefficient, $\eta$ the efficiency factor for chromium reduction with respect to substrate utilization, $\lambda$ the proportionality constant which accounts for the differences in the microbial activity in a suspended batch system and attached continuous system. It also implicitly accounts for metabolic retardation due to starving in the stabilization and acclimatization periods. In the present model, the pore velocity, $u$ is obtained by dividing the Darcy velocity, $U$ by the porosity of the soil column, $\theta$. The coefficient of dispersion, $D$ is obtained by multiplying the pore velocity, $u$ with the dispersivity, $\alpha_L$. Computation of the retardation coefficients for hexavalent chromium and substrate is based on the equilibrium adsorption studies. Constant 0.63 in Eq. (7) was obtained from batch studies.

The basic assumptions made in deriving the model can be summarized as follows:

1. The flow in the column is one-dimensional.
2. The porous medium is homogeneous, and the porosity remains constant through out the study period.
3. Adsorption is assumed to occur under equilibrium conditions.
4. The model is based on the "macroscopic modeling" of microbiological reactions. This is a single phase model where all the microorganisms present in a given control volume are equally exposed to the substrate concentration prevailing in the bulk liquid volume [24].
5. The microbes are immobile.
6. The contaminant is toxic and has inhibitory effect on microbial growth rate.
7. The Monod's equation with inhibition describes the microbial growth.
8. Only a fraction of substrate is available for Cr(VI) reduction.
9. Cr(III) generated due to biotransformation is either adsorbed or precipitated and retained on the soil matrix.
10. The temperature is constant.

Table 3
Isotherm constants for soil adsorption

| | Freundlich isotherm | | |
|---|---|---|---|
| | $K_f$ | $1/n$ | $r^2$ |
| Sand | | | |
| Cr(VI) | 0.006638 | 0.835 | 0.90 |
| Cr(III) | 0.06723 | 0.4582 | 0.88 |
| Li | 0.005643 | 0.829 | 0.96 |
| Soil A | | | |
| Cr(VI) | 0.01798 | 0.9445 | 0.98 |
| Cr(III) | 2.9 | 0.339 | 0.96 |
| Li | 0.068061 | 0.5128 | 0.96 |
| Cr(VI) in presence of molasses and lithium | | | |
| Soil C | 0.036694 | 0.7742 | 0.96 |
| Sand | 0.010325 | 1.0512 | 0.94 |
| Soil A | 0.012303 | 1.9135 | 0.96 |
| Molasses in presence of Cr(VI) and lithium | | | |
| Soil C | 0.044545 | 0.7861 | 0.87 |
| Sand | 0.050687 | 0.7575 | 0.90 |
| Soil A | 0.055017 | 0.764 | 0.95 |
| Cr(III) in presence of molasses and lithium (pH 7.0) | | | |
| Soil C | 0.1411 | 4.438 | 0.928 |
| Sand | 0.734 | 5.778 | 0.933 |
| Soil A | 0.1667 | 4.628 | 0.859 |
| Cr(III) in presence of molasses and lithium (pH 4.0–5.0) | | | |
| Sand | 0.0257 | 0.8443 | 0.983 |
| Soil A | 0.1979 | 0.704 | 0.855 |

A direct numerical substitution approach with Picard iteration was used to solve the non-linear partial differential equations [25–27]. Advection-dispersion part was discretized using the implicit–explicit approach for time discretization because of its better numerical stability and accuracy. The spatial discretization for advection term was based on an Essentially Non-Oscillating scheme in which MINMOD limiter was employed for suppressing numerical oscillations. A central difference scheme was used for spatial discretization of the dispersive term.

## 4. Results and discussion

### 4.1. Batch studies

Batch studies were conducted to determine the equilibrium adsorption constants, and the biokinetic parameters for bacterial growth. Adsorption equilibrium studies were conducted for Cr(VI), Cr(III), Li, and COD (molasses) for all the three soils. Adsorption studies were also conducted for Cr(VI) and Cr(III) in presence of COD and Li to understand the interference of these components on adsorption. Freundlich isotherm was used for fitting the experimental data. Table 3 shows the Freundlich coefficient ($K_f$), exponent ($1/n$) and the corresponding correlation coefficient for all the isotherms [17]. It can be seen that adsorp-

Table 4
Modified coefficients of efficiency ($E$) for the transport and biotransformation studies

| Soil type | Initial pore velocity (cm/h) | Bacterial conc. added (mg/g) | Column length (cm) | Cr(VI) | | | | | Substrate | | | | Lithium | | | | |
|---|---|---|---|---|---|---|---|---|---|---|---|---|---|---|---|---|---|
| | | | | 20 | 40 | 60 | 80 | 49 | 20 | 40 | 60 | 80 | 49 | 20 | 40 | 60 | 80 | 49 |
| Soil C | 7.32 | 0.0232 | 100 | 0.398 | 0.649 | 0.702 | 0.8272 | | 0.24 | 0.56 | 0.497 | 0.56 | | 0.745 | 0.87 | 0.93 | 0.96 | |
| Sand | 6.67 | 0.0205 | 100 | 0.784 | 0.712 | 0.918 | 0.9496 | | 0.823 | 0.66 | 0.743 | 0.88 | | 0.828 | 0.93 | 0.87 | 0.75 | |
| Sand | 1.16 | 0.0405 | 100 | 0.778 | 0.557 | 0.345 | −0.319 | | 0.576 | 0.849 | 0.862 | 0.79 | | 0.933 | 0.89 | 0.77 | 0.67 | |
| Soil A | 5.833 | 0.0205 | 100 | −0.365 | −1.616 | −6 | −10.096 | | 0.45 | 0.615 | 0.515 | 0.44 | | −0.1 | −0.2 | −0.9 | −0.6 | |
| Bio-barrier study | | | | | | | | | | | | | | | | | | |
| Soil A | 1.98 | 0.0205 | 10[a] | 0.074 | 0.14 | −0.25 | 0.0697 | 0.21 | 0.084 | 0.462 | 0.461 | 0.49 | 0.64 | 0.771 | 0.88 | 0.96 | 0.94 | 0.82 |
| Soil A | 2.66 | 0.205 | 10[a] | 0.833 | 0.766 | −0.46 | −2.4112 | 0.69 | 0.75 | 0.863 | 0.616 | 0.84 | 0.94 | 0.887 | 0.93 | 0.87 | 0.96 | 0.86 |

[a] Bio-barrier thickness (cm).

tion of Cr(III) is much higher than Cr(VI). Adsorption of Li is almost negligible, indicating that it is a conservative pollutant, which serves as a tracer to determine dispersion characteristics.

### 4.2. Studies to estimate biokinetic parameters

Biotransformation studies were conducted with initial chromium concentrations of 0, 1, 5, 10, 20, 50, 100, 200, 300, and 500 mg/L. Bacterial cells (36 mg/L) were added to the media and hexavalent chromium, COD and bacterial concentrations were measured at various time intervals. $\mu_{max}$ and $K_s$ were determined using the data from experiments conducted without chromium, and with an initial molasses concentration of 5000 mg/L as COD. The bacterial growth in the exponential phase was fitted to the equation $M = M_0 e^{\mu_{max} t}$, where $M_0$ is the initial biomass concentration. Using this $\mu_{max}$ value, the $K_s$ value was determined such that the simulated growth curve matched with the experimental growth curve. $K_i$ was then determined using the experiments for microbial growth rate in the presence of chromium, using Monod's equation with inhibition. The biokinetic parameters obtained are: $\mu_{max} = 0.3\ h^{-1}$, $K_s = 40.0$ mg/L (as COD), $K_i = 3.05$ mg/L of Cr(VI), and $Y = 0.263$.

The efficiency factor, $\eta$, i.e. ratio between amount of Cr(VI) biotransformed to the amount of molasses consumed, as well as $\lambda$ were determined by back-fitting the Cr(VI) breakthrough curve at port 20 cm using Genetic Algorithms. The same values were used in the mathematical simulations for breakthrough curves of Cr(VI), and molasses at all other ports located at 40, 60, and 80 cm. $\lambda$-values were 0.1, 0.065, and 0.1 for Soils A, sand, and soil C, respectively, whereas estimated value of $\eta = 0.3$, which is almost the same as reported in the literature [16].

### 4.3. Transport studies with no biotransformation

It is essential to understand the transport of Cr(VI) without any biotransformation in order to study the role of biotransformation in the containment of Cr(VI) in aquifers, considering only adsorption. These studies would help in validating the numerical solution of the advection-dispersion-adsorption part of the mathematical model. In this study, the model performance was statistically evaluated using the dimensionless modified coefficient of efficiency, $E$ [28,29].

$$E = 1 - \frac{\sum_{i=1}^{N} [|E(t_i) - O(t_i)|]}{\sum_{i=1}^{N} |O(t_i) - \bar{O}|} \tag{10}$$

where $E(t_i)$ is the numerically simulated value of a variable at time $t_i$, $O(t_i)$ the observed value of the same variable at time $t_i$, and $\bar{O}$ is the mean value of the observed variable. $E$ varies between $-\infty$ and 1.0, the higher values indicating better model prediction. As suggested by Köhne et al. [29] a positive value of $E$ represents an "acceptable" simulation whereas $E > 0.5$ represents a "good" simulation. $E$ equal to one indicates a "perfect" simulation. Values of $E$ for all the simulations carried out in this study are presented in Table 4.

Numerically simulated results along with the experimental data for the breakthrough of Cr(VI) at 20, 40, 60, and 80 cm

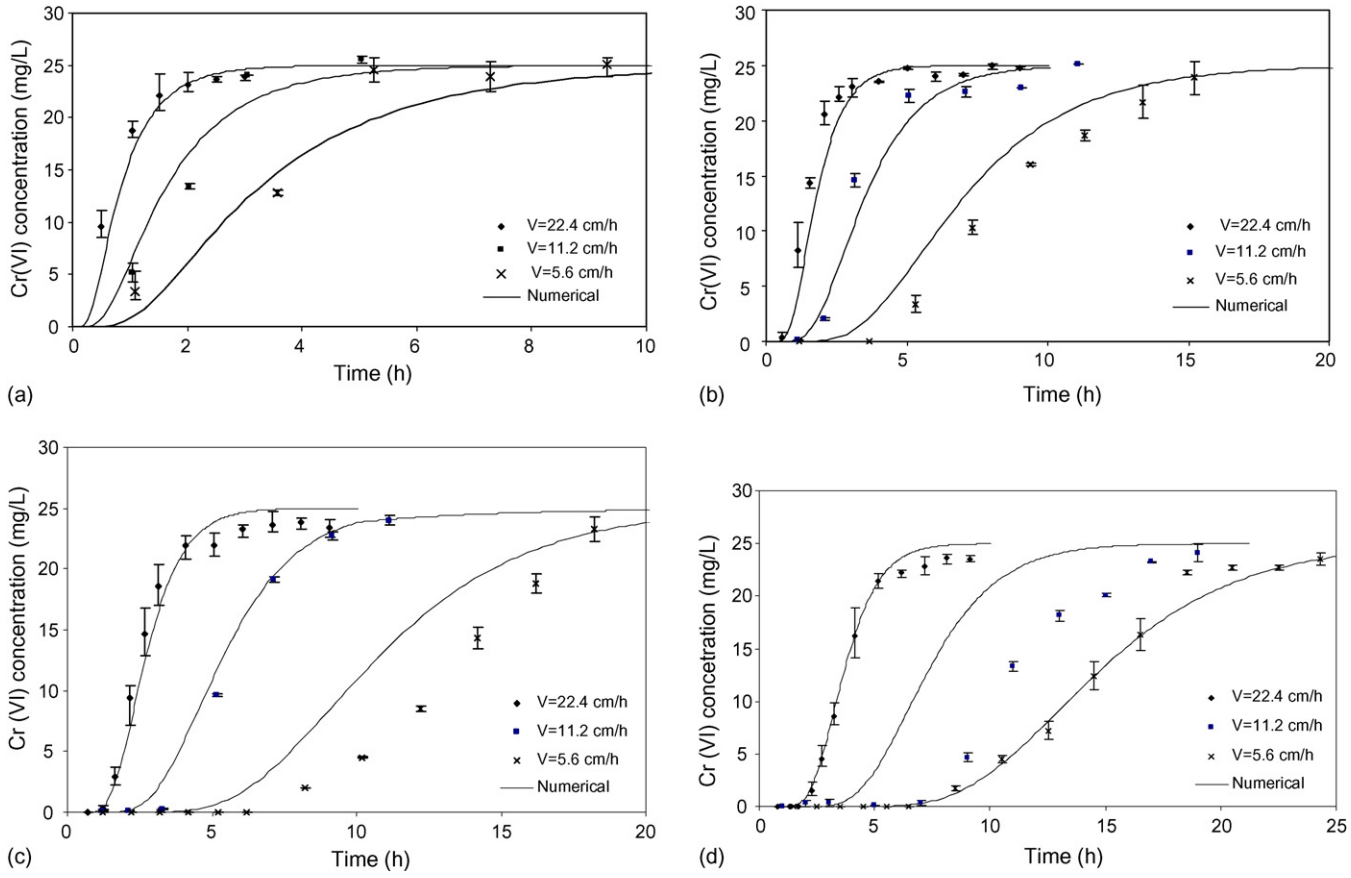


Fig. 2. Experimental and numerical Cr(VI) breakthrough curves of Soil A column for different pore velocities; no biotransformation (pH 6.7–7, inlet Cr(VI) concentration 25 mg/L): (a) $x = 20$ cm, (b) $x = 40$ cm, (c) $x = 60$ cm), and (d) $x = 80$ cm.

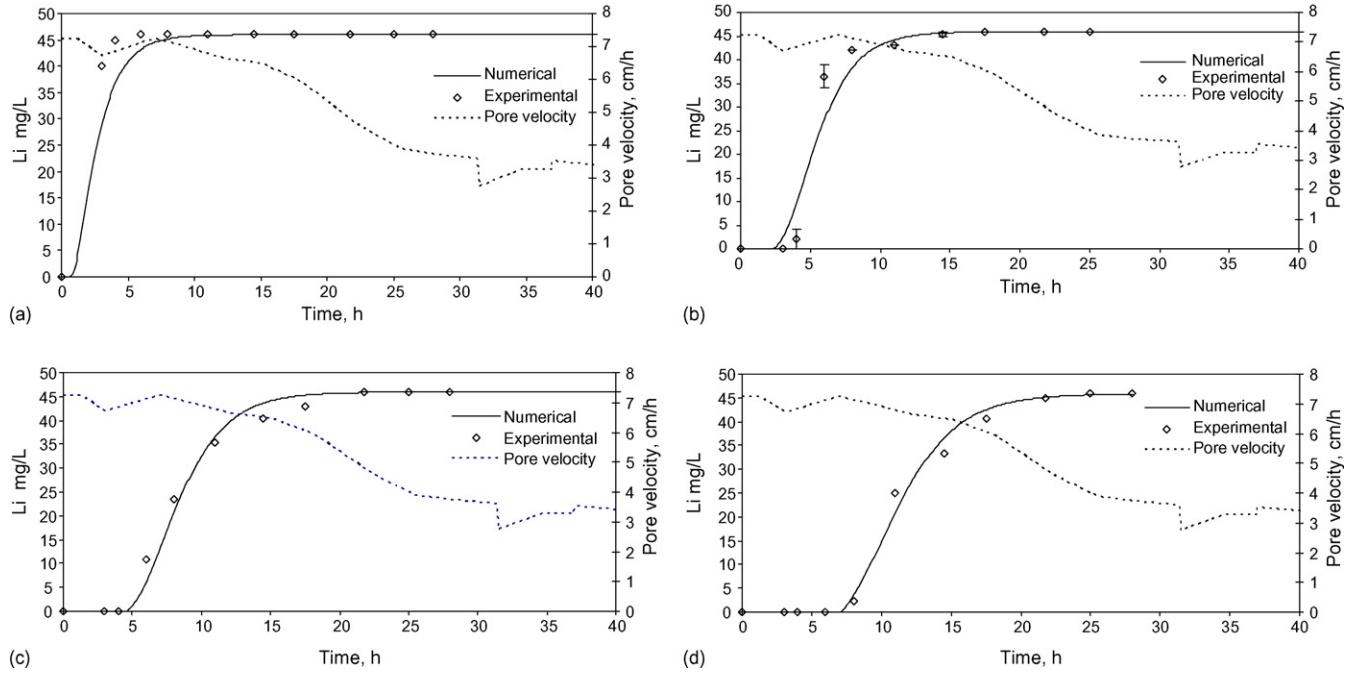


Fig. 3. Experimental and numerical lithium breakthrough curves of Soil C column; with biotransformation (pH 6.2–7.2, inlet Lithium concentration 46 mg/L): (a) $x = 20$cm, (b) $x = 40$ cm, (c) $x = 60$ cm, and (d) $x = 80$ cm.

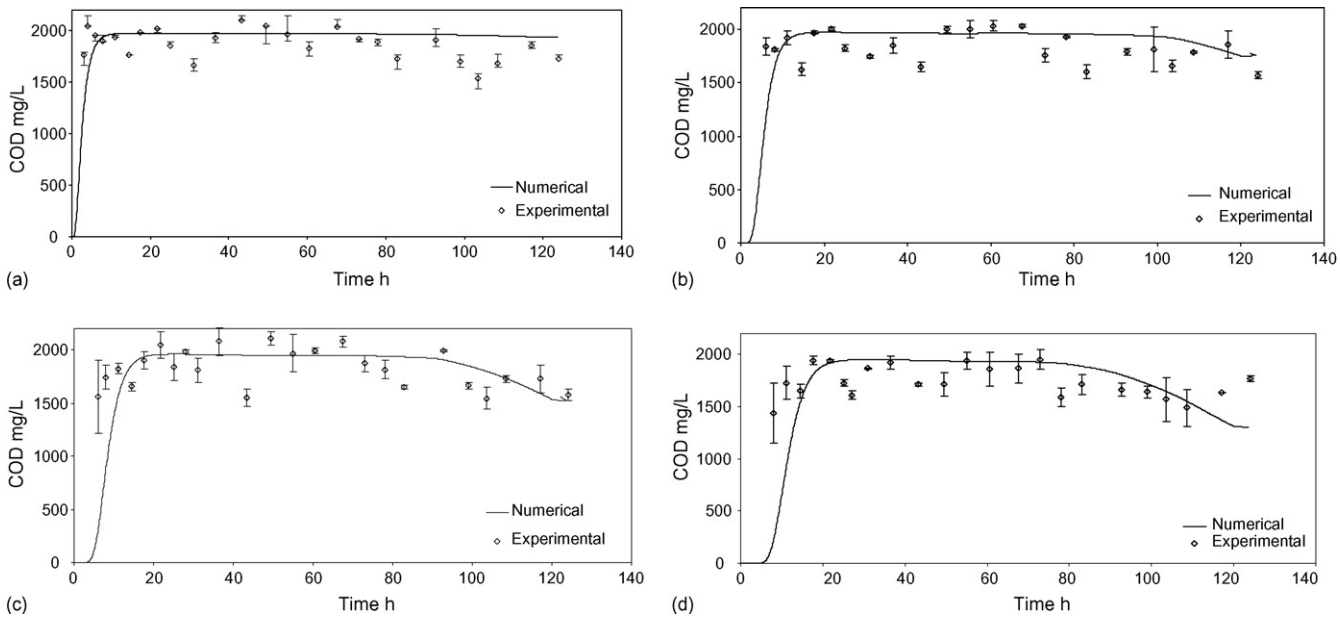


Fig. 4. Experimental and numerical substrate breakthrough curves of Soil C column; with biotransformation (pH 6.2–7.2, inlet COD concentration 2000 mg/L): (a) $x = 20$cm, (b) $x = 40$ cm, (c) $x = 60$ cm, and (d) $x = 80$ cm.

ports, for three pore velocities in column with Soil A are presented in Fig. 2a–d. The measured breakthrough data at 20 cm port was used to back fit the dispersivity, $\alpha_L$, and the same was used to simulate the breakthrough curves at other ports. The dispersivity in these studies was equal to 4.46 cm, and the dispersion coefficient varied linearly with pore velocity. Dimensionless modified coefficient of efficiency, $E$ for these simulations (Table 4) varied from 0.54 to 0.94 indicating that the mathematical model simulates the experiments well, which is also evident from Fig. 2a–d. However, there was disparity between the model and experimental results for the case of $v = 5.6$ cm/h at $x = 60$ cm ($E = 0.54$), although the matching was

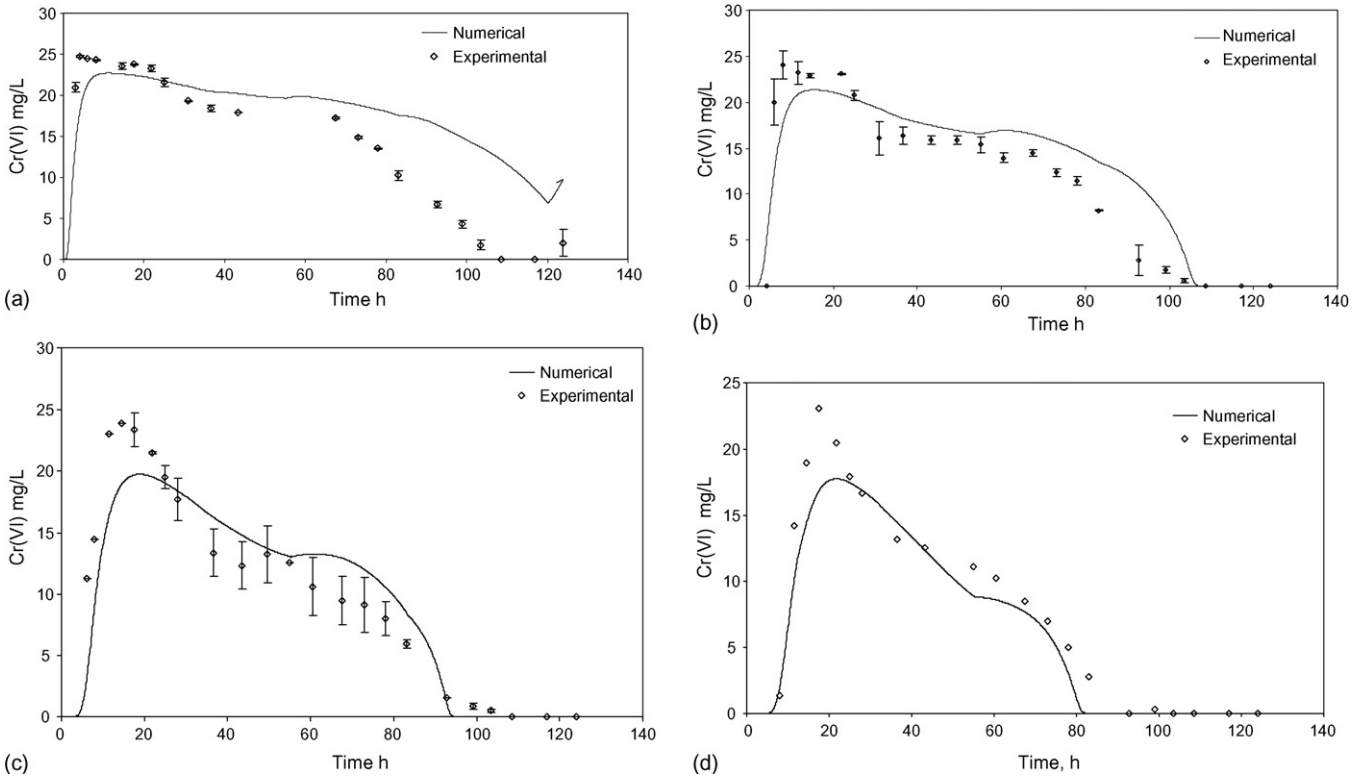


Fig. 5. Experimental and numerical Cr(VI) breakthrough curves of soil C column; with biotransformation (pH 6.2–7.2, inlet Cr(VI) concentration 25 mg/L): (a) $x = 20$ cm, (b) $x = 40$ cm, (c) $x = 60$ cm, (d) $x = 80$ cm.

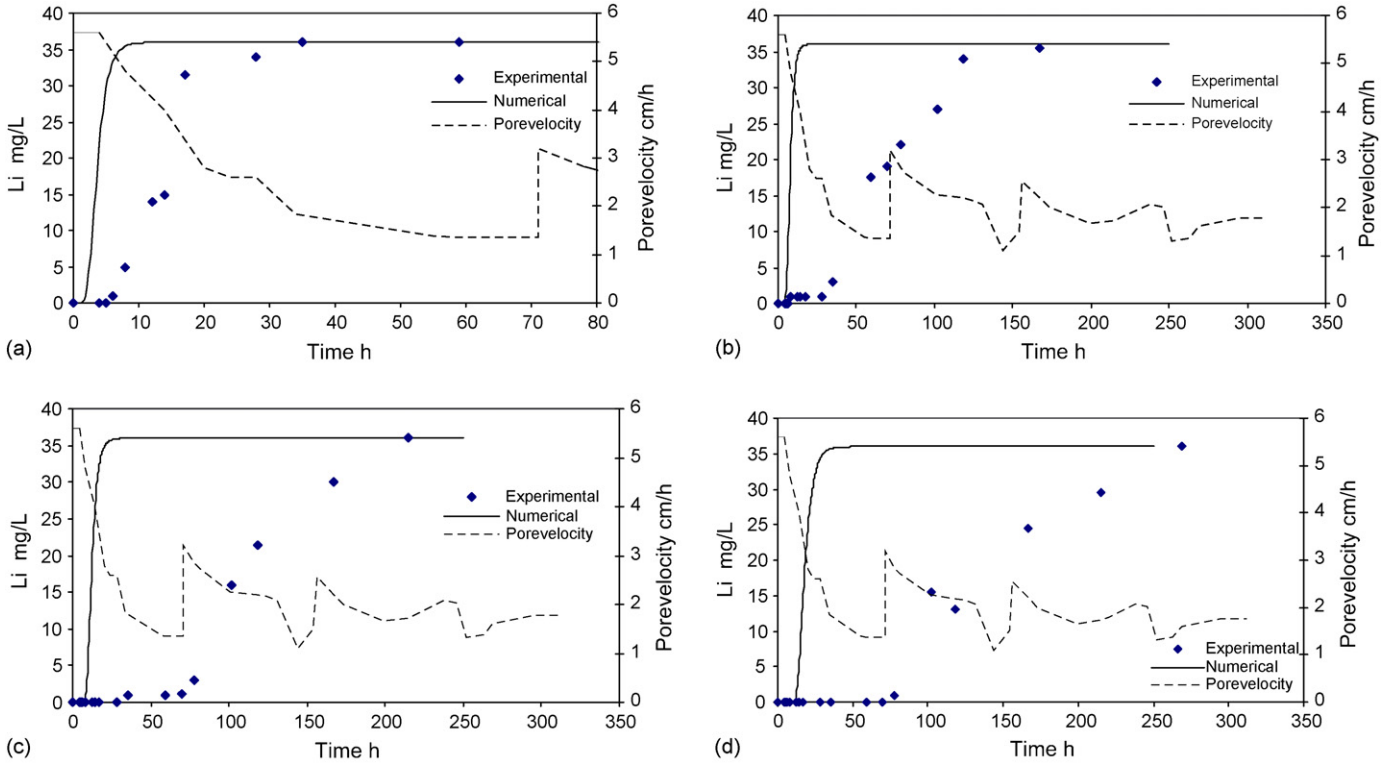


Fig. 6. Experimental and numerical lithium breakthrough curves of soil A column; with biotransformation (pH 6.2–7.2, inlet Li concentration 36 mg/L): (a) $x = 20$ cm, (b) $x = 40$ cm, (c) $x = 60$ cm, (d) $x = 80$ cm.

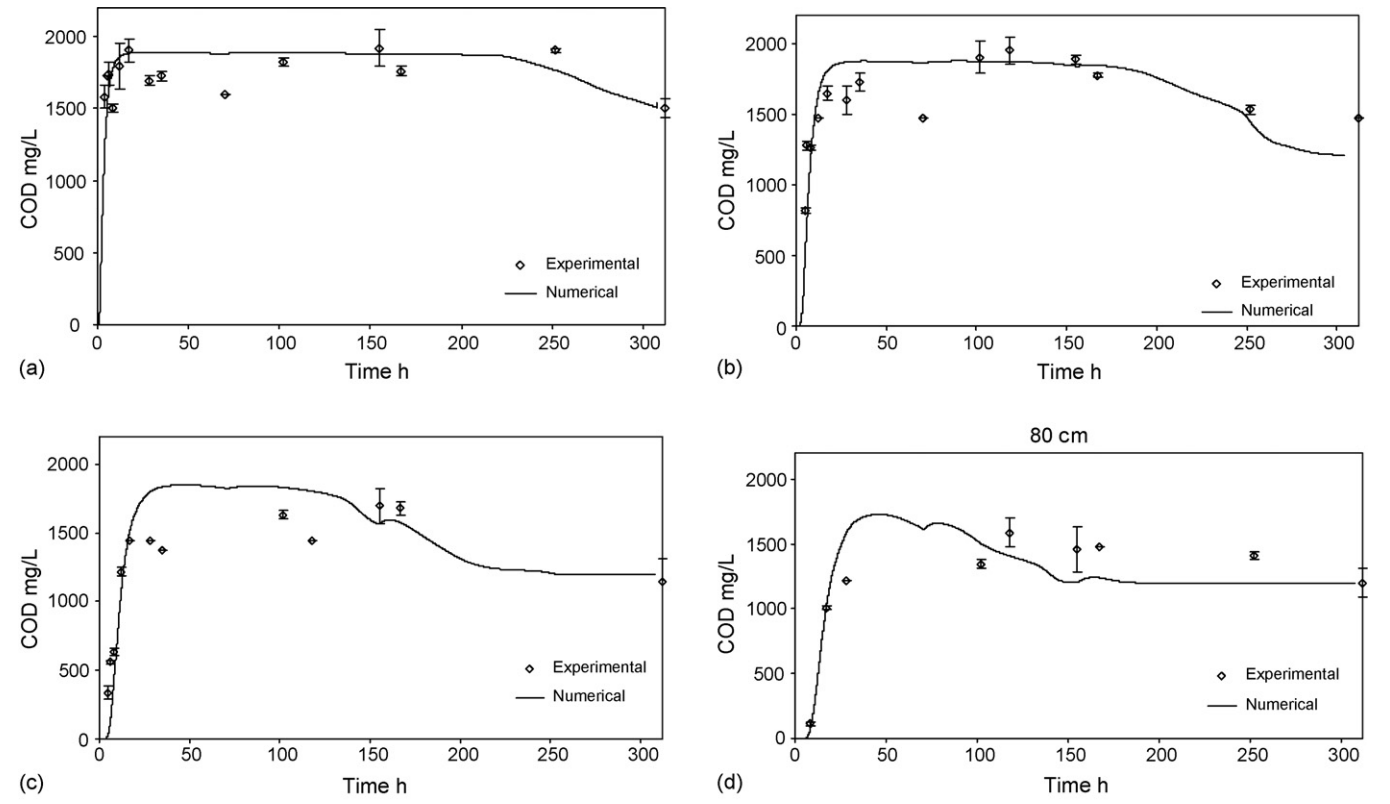


Fig. 7. Experimental and numerical substrate breakthrough curves of Soil A column; with biotransformation (pH 6.2–7.2, inlet COD concentration 2000 mg/L): (a) $x = 20$cm, (b) $x = 40$ cm, (c) $x = 60$ cm, and (d) $x = 80$ cm.

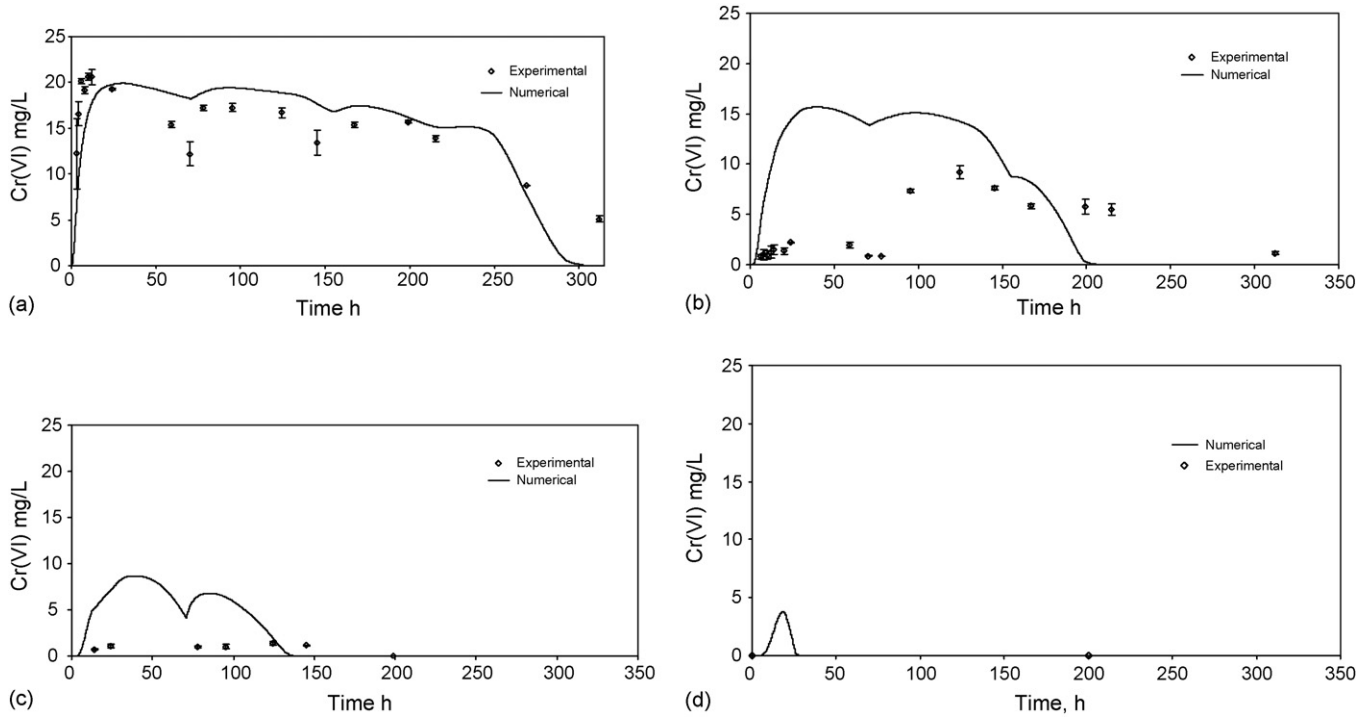


Fig. 8. Experimental and numerical Cr(VI) breakthrough curves of soil A column; with biotransformation (pH 6.2–7.2, inlet Cr(VI) concentration 25 mg/L): (a) $x = 20$ cm, (b) $x = 40$ cm, (c) $x = 60$ cm, (d) $x = 80$ cm.

good at $x = 80$ cm ($E = 0.94$). One would expect that the disparity between the simulated and observed data to increase in the direction of transport due to retardation. Here, it may be noted that a single dispersion coefficient was used for the entire column. On the other hand, the dispersion coefficient may be varying spatially due to non-homogeneity in compaction. This is especially true in case of soil with high clay content (Soil A). It is also obvious from these results that adsorption alone was not able to

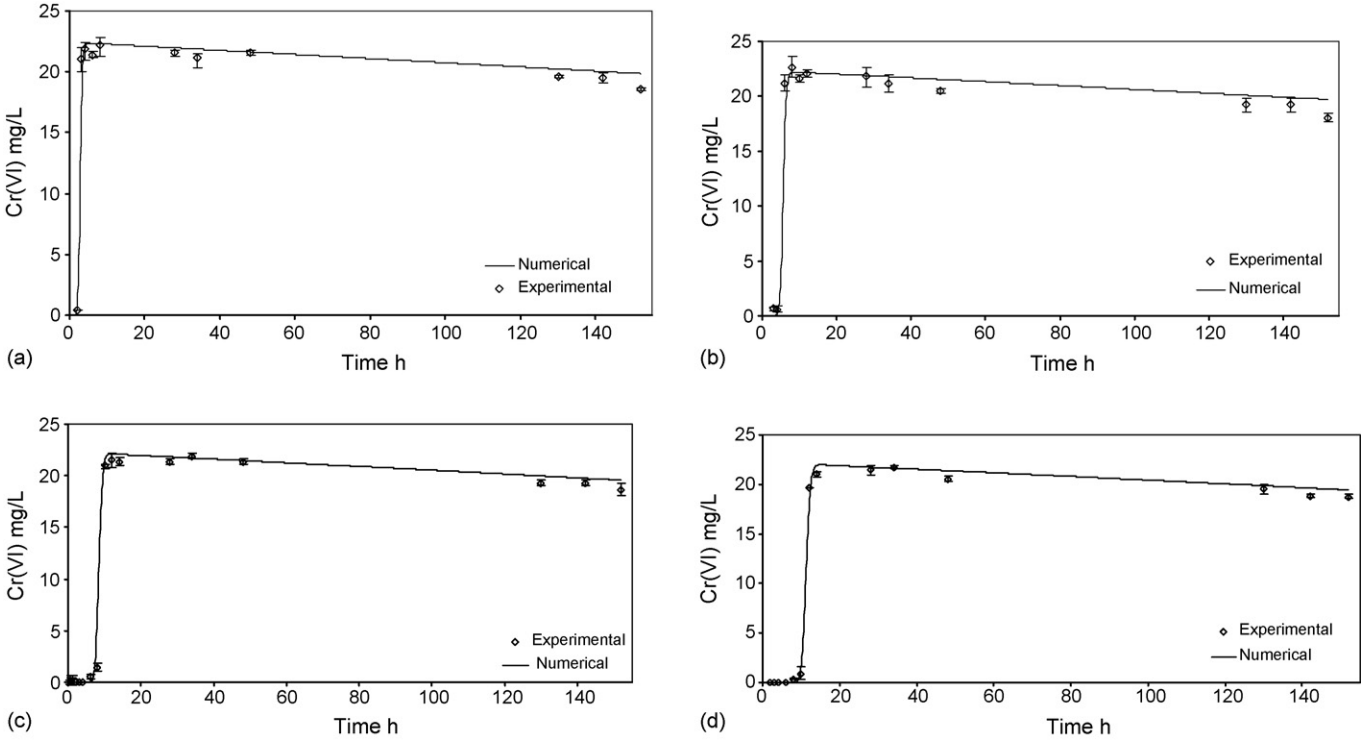


Fig. 9. Experimental and numerical Cr(VI) breakthrough curves of sand column; with biotransformation (pH 6.2–7.2, inlet Cr(VI) concentration 25 mg/L, pore velocity 6.67 cm/h): (a) $x = 20$cm, (b) $x = 40$ cm, (c) $x = 60$ cm, and (d) $x = 80$ cm.

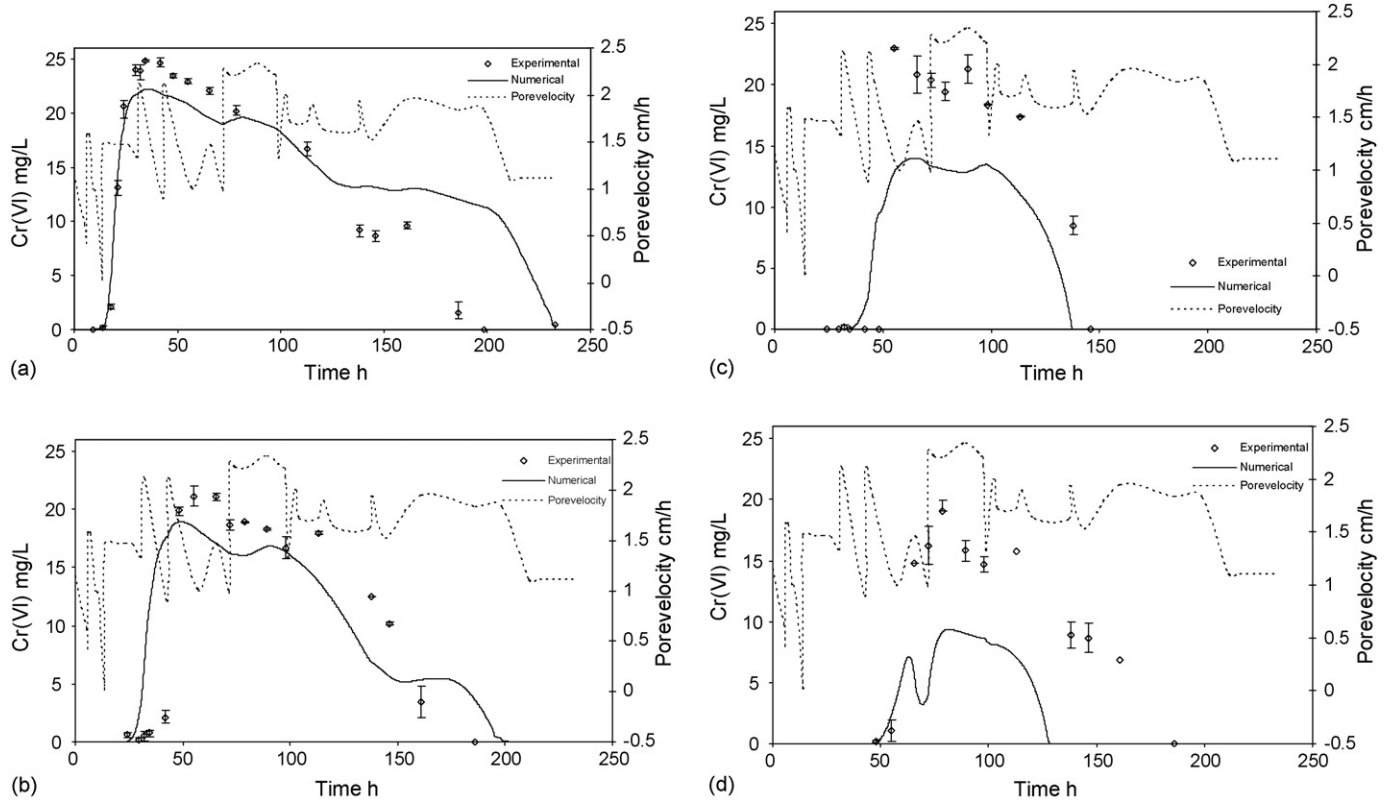


Fig. 10. Experimental and numerical Cr(VI) breakthrough curves of sand column; with biotransformation (pH 6.2–7.2, inlet Cr(VI) concentration 25 mg/L, pore velocity 1.16 cm/h): (a) $x = 20$ cm, (b) $x = 40$ cm, (c) $x = 60$ cm, and (d) $x = 80$ cm.

contain Cr(VI) in the aquifer. The maximum Cr(VI) concentration at 80 cm port was almost equal to the inlet concentration irrespective of pore velocity.

### 4.4. Transport studies with biotransformation

Bench scale experiments were conducted for transport along with biotransformation in saturated, confined aquifer systems. As given in Table 2, experiments were conducted for two different soils (Soils A and C), and for sand. For sand, experiments were conducted for two different pore velocities.

Fig. 3a–d shows the comparison between the numerically simulated and experimentally measured breakthrough for lithium tracer at $x = 20, 40, 60$, and 80 cm, for transport in column with Soil C. This figure also shows the pore velocity variation with time. Pore velocity was obtained from the measured Darcy velocity by dividing it with porosity. It was assumed that the porosity remained constant, though it might have changed. It can be seen from Fig. 3 that the pore velocity was decreasing drastically as the time progressed. Periodically the head in the upstream tank was adjusted to increase the velocity to reasonable levels. Similar trend in the reduction of pore velocity with time was observed in all the other experiments also. The pore velocities reported here were used as velocity input for the solution of transport equations in all simulations. Fig. 4a–d shows the comparison between the numerically simulated and experimentally measured breakthrough for substrate (molasses) at $x = 20$, 40, 60, and 80 cm, for the same experiment. Fig. 5a–d shows the same for Cr(VI). In the numerical simulations for the transport of Cr(VI) and molasses, the biokinetic parameters as determined from the batch experiments were used. The dispersivity value was equal to 3.5 cm. This value was obtained by fitting the breakthrough curves for lithium tracer at $x = 20$, 40, 60, and 80 cm, since the lithium transport gives the hydraulic characterization. $E$ values for these simulations varied from 0.75 to 0.96, indicating that the parameter estimation for dispersivity using the lithium breakthrough data was good. As mentioned earlier, a parameter $\lambda$ has been introduced in the model to account for the differences in the microbial growth in a suspended batch system and attached continuous system. It also implicitly accounts for metabolic retardation due to starving in the stabilization and acclimatization periods. It was assumed that this parameter $\lambda$ was constant through out the column. Therefore, the chromium breakthrough curve at $x = 20$ cm was used to back fit the value of this parameter ($E = 0.4$), and the same was used for simulating the substrate and chromium breakthrough curves at the remaining ports. This value was equal to 0.1. Fig. 4a–d shows that simulation of molasses transport was satisfactory ($E$ value varied from 0.24 to 0.56). It can also be seen that numerically simulated breakthrough curves for hexavalent chromium at $x = 40$, 60, and 80 cm match well with the experimental data ($E = 0.65$, 0.70, and 0.83). It can be inferred from these results that the proposed model is able to explain the transport and biotransformation of hexavalent chromium in the confined aquifer. One calibrating parameter, $\lambda$ was able to implicitly include most of

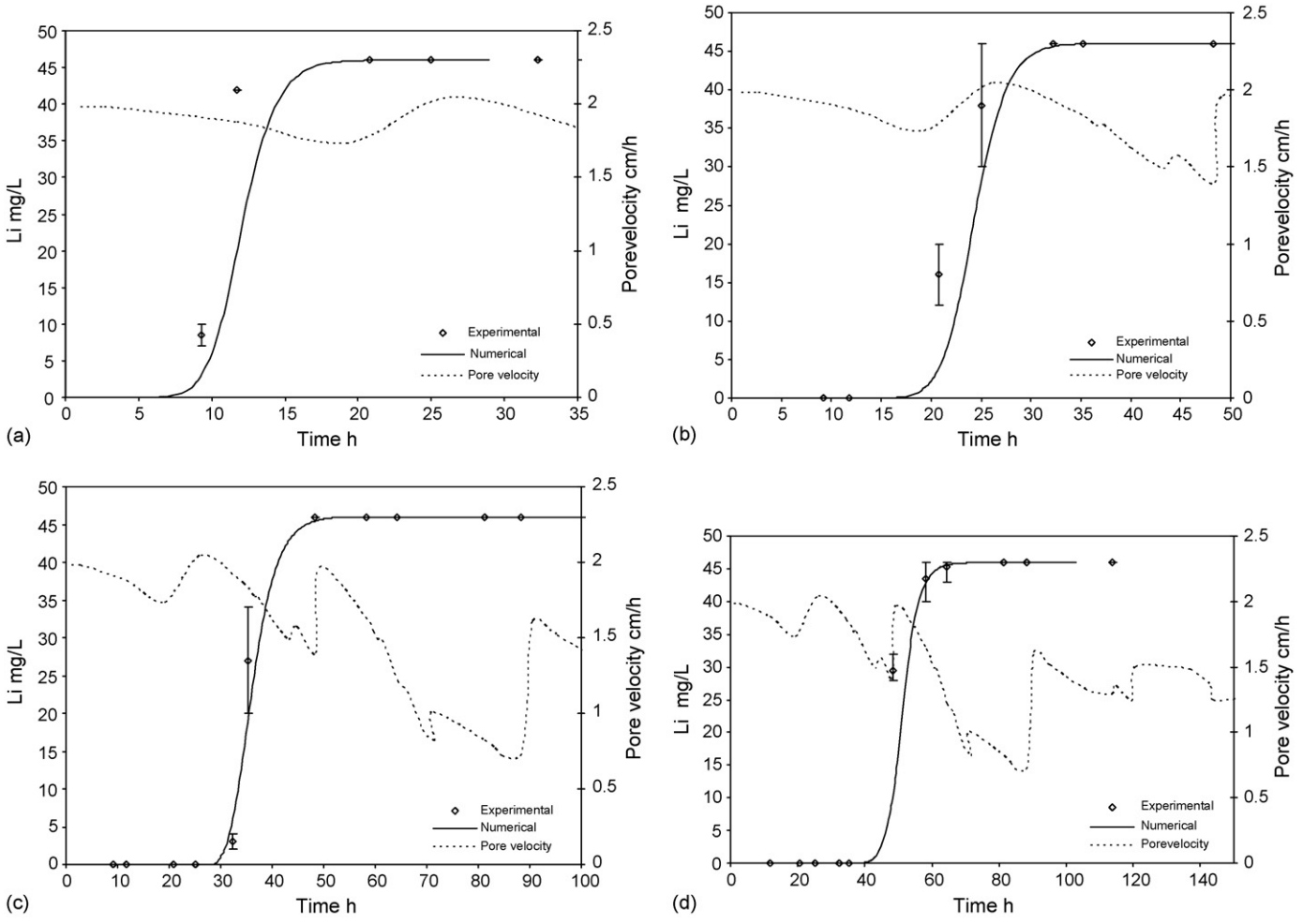


Fig. 11. Experimental and numerical lithium breakthrough curves of BB1; (pH 6.2–7.2, inlet Li concentration 46 mg/L, pore velocity 1.6 cm/h): (a) $x = 20$ cm, (b) $x = 49$ cm, (c) $x = 60$ cm, and (d) $x = 80$ cm.

the uncertainties associated with biotransformation in a confined silty aquifer.

Experimental results for Cr(VI) breakthrough indicate that there was a high concentration of Cr(VI) initially at all the ports, which was due to dominance of advection as compared to the biotransformation. Subsequently, the microbial activity increased due to an increase in the microbial population, which resulted in significant Cr(VI) reduction. This trend was well simulated by the mathematical model.

Figs. 6–8 show the numerically simulated and experimental breakthrough curves for lithium, molasses, and hexavalent chromium, respectively, for Soil A with 6.19% clay content. The same value of λ as obtained for Soil C was used in this case also. Dispersivity in this experiment, as obtained from the lithium breakthrough data, was equal to 4.46 cm. *E* values for these simulations varied from −0.9 to −0.1, indicating that the parameter estimation for dispersivity using the lithium breakthrough data was not satisfactory. It is clear from these figures that as the clay content increases, it becomes difficult to simulate even the transport of lithium, which is a conservative pollutant. The *E* values for Cr(VI) simulations varied from −10.1 to −0.37, again indicating an unsatisfactory performance by the mathematical model. However, the simulation of molasses transport was satisfactory (*E* values ranged from 0.44 to 0.62), may be because of high concentrations. It may be noted that more than 80% of molasses was left even after the complete biotransformation of Cr(VI). The gas released due to microbial metabolic activity might have been trapped unevenly in the column and introduced non-homogeneities. These non-homogeneities affected the dispersivity with respect to time, which was not accounted in the present model. It may be noted here that, for the same soil without biotransformation, transport of both lithium and Cr(VI) were simulated well by the proposed model. Thus, it may be concluded that for modeling the transport and biotransformation of Cr(VI) in aquifers with high clay content, non-homogeneities introduced by biotransformation process and the consequent changes in the hydro-geological conditions should be considered for a better simulation.

Figs. 9a–d and 10a–d present the breakthrough for Cr(VI) at 20, 40, 60, and 80 cm ports for the case of transport and biotransformation experiments in sand, for two different velocities of 6.67 and 1.16 cm/h, respectively. Dispersivities in these experiments (as obtained using the lithium tracer data, results not presented) were 0.1 and 0.3 cm, respectively. The *E* values

for lithium transport in the case of velocity of 6.67 cm/h varied from 0.75 to 0.93. They varied from 0.67 to 0.93 when the velocity was equal to 1.16 cm/h. The λ value (as obtained from the Cr(VI) breakthrough data at $x = 20$ cm) was 0.065. It is very clear that the effect of biotransformation on Cr(VI) containment is very significant in the case of low pore velocity. In case of high pore velocity, breakthrough of Cr(VI) occurred much earlier and also the maximum concentration was almost equal to the inlet concentration even after 150 h. These effects are well simulated by the mathematical model as evident from the figures ($E$ values ranged from 0.71 to 0.95). Pore velocity had a significant effect on bacterial retention on the soil matrix. High pore velocity resulted in significant bacterial cell washout from 0.021 to 0.005 mg/g, while the bacterial concentration reduced from 0.04 to 0.027 mg/g in the case of column with low pore velocity. It can be seen from Fig. 10a–d that the rate of Cr(VI) containment increased with respect to time because of corresponding increase in biomass concentration in the system. Increased microbial activity in the case of low pore velocity might have introduced some non-homogeneity and had affected the hydrogeology. As a result, the performance of the mathematical model was not as good as in the case of high pore velocity ($E$ values ranged from 0.78 to −0.32).

To summarize, comparison of the mathematical model and experimental data for Soils A, C, and sand shows that in case of sand, the prediction of breakthrough curves was more accurate. This may be due to more homogeneity in the case of sand, compared to that of Soils A and C, which contained various levels of clay and silt. Uneven accumulation of gas generated due to biotransformation might have also introduced considerable non-homogeneity in case of clayey soils. This effect was not considered in the simple mathematical model. The mathematical model did not consider the change in the dispersivity due to microbial activity. It may be also noted that we used the same value of porosity to determine the pore velocity from the measured Darcy velocity. Non-uniform entrapment of gas might have resulted in non-uniformity in pore velocity. This effect was also not considered in the present model.

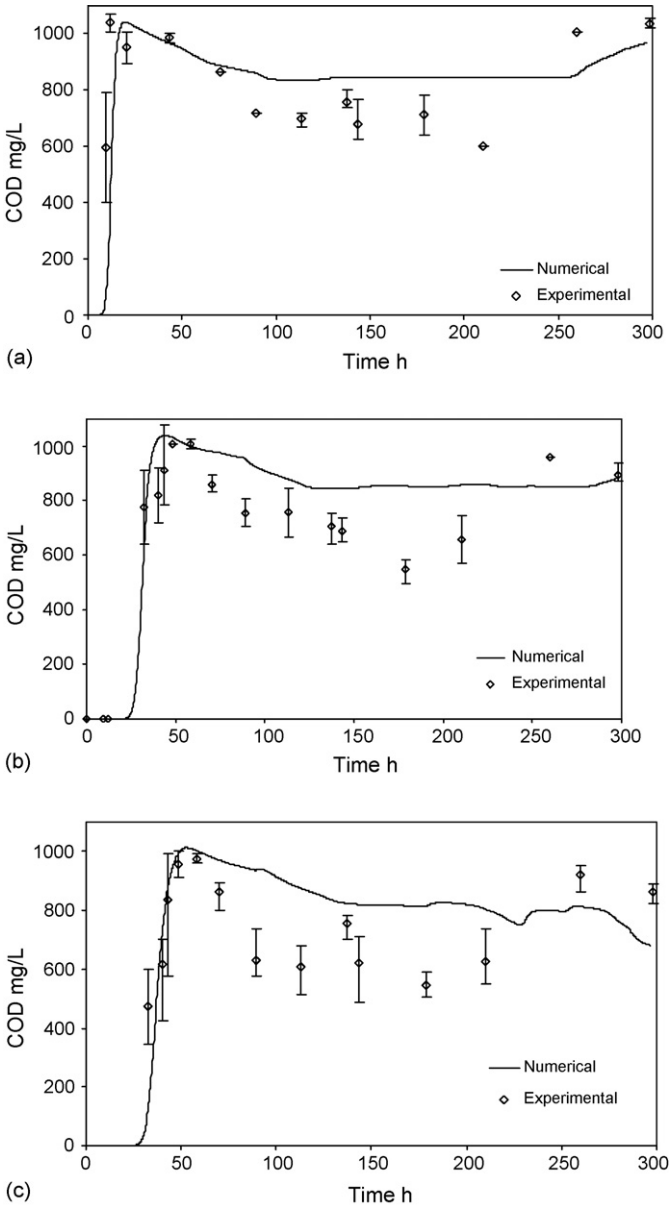


Fig. 12. Experimental and numerical substrate breakthrough curves of BB1; (pH 6.2–7.2, inlet COD concentration 1000 mg/L, pore velocity 1.6 cm/h): (a) $x = 20$cm, (b) $x = 49$ cm, and (c) $x = 60$ cm.

### 4.5. Transport and biotransformation studies with bio-barriers

As given in Table 2, two experiments were conducted with a bio-barrier in place from $x = 50$ to $x = 60$ cm. In these experiments, Soil A was used for the bio-barrier, while sand was used in the rest of the column. Initial bacterial concentration in Bio-barrier one (BB1) was 0.0205 mg/g of soil while it was 0.205 mg/g in BB2. Breakthrough curves for lithium for BB1 at 20, 49, 60, and 80 cm are presented in Fig. 11a–d. The breakthrough, curves for molasses and Cr(VI) for the same ports are given in Figs. 12 and 13, respectively. Breakthrough curves for lithium, molasses and Cr(VI) at 20, 49, and 60 cm for BB2 are presented in Figs. 14–16. It can be seen from these figures (Figs. 13 and 16) that the 10 cm bio-barrier was able to contain the hexavalent chromium, even when the inlet chromium concentration was as high as 25 mg/L. Also, the pore velocity (1.6 cm/h) in these experiments was quite high compared to pore velocities normally encountered in the field. The chromium containment was almost complete in BB2, in which the initial microbial concentration was relatively high. From this, it can be concluded that bio-barrier using enriched microbes is a viable method for the remediation of chromium contaminated aquifers.

Table 5 shows the input values for various parameters used in the mathematical simulations for the bio-barrier experiments. In these experiments, measurement of bacterial concentration in the outlet reservoir showed that there was considerable bacterial washout during the stabilization period. Assuming that washout had occurred uniformly from the bio-barrier and there was no retention of washed out biomass in the down stream column, the initial biomass concentration for biotransformation of Cr(VI) in the bio-barrier was estimated as 0.0205 mg/g in BB1

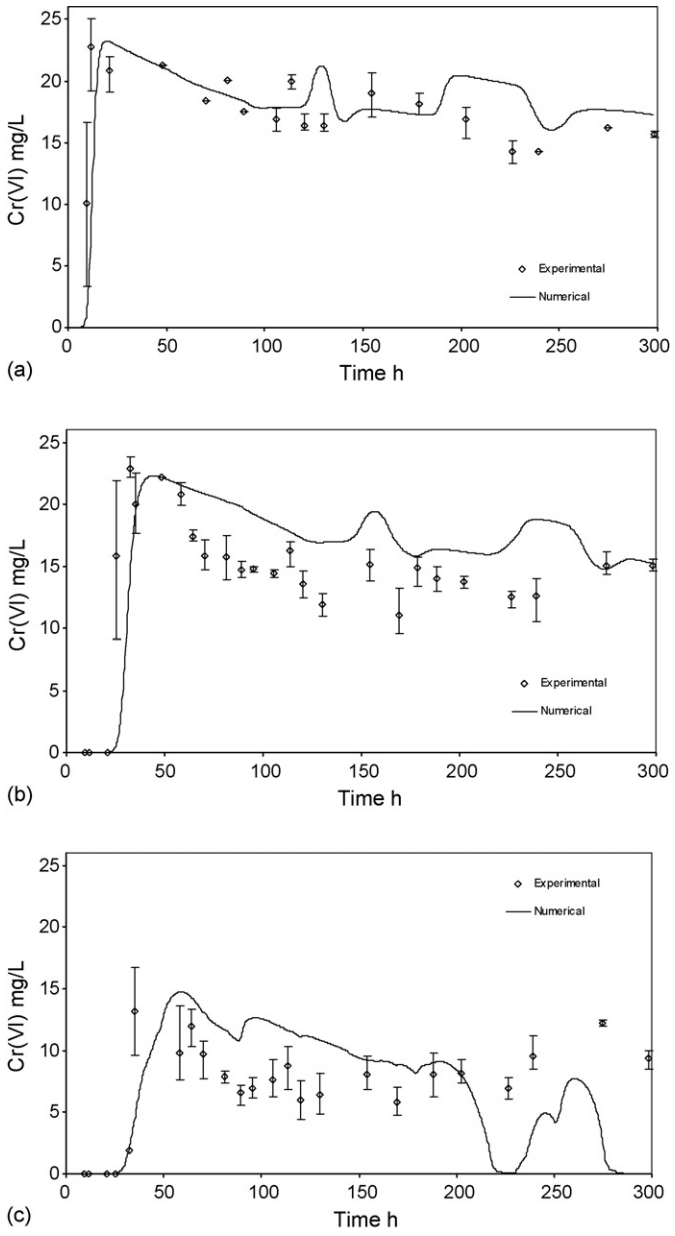


Fig. 13. Experimental and numerical Cr(VI) breakthrough curves of BB1; (pH 6.2–7.2, inlet Cr(VI) concentration 25 mg/L, pore velocity 1.6 cm/h): (a) $x = 20$ cm, (b) $x = 49$ cm, (c) $x = 60$ cm.

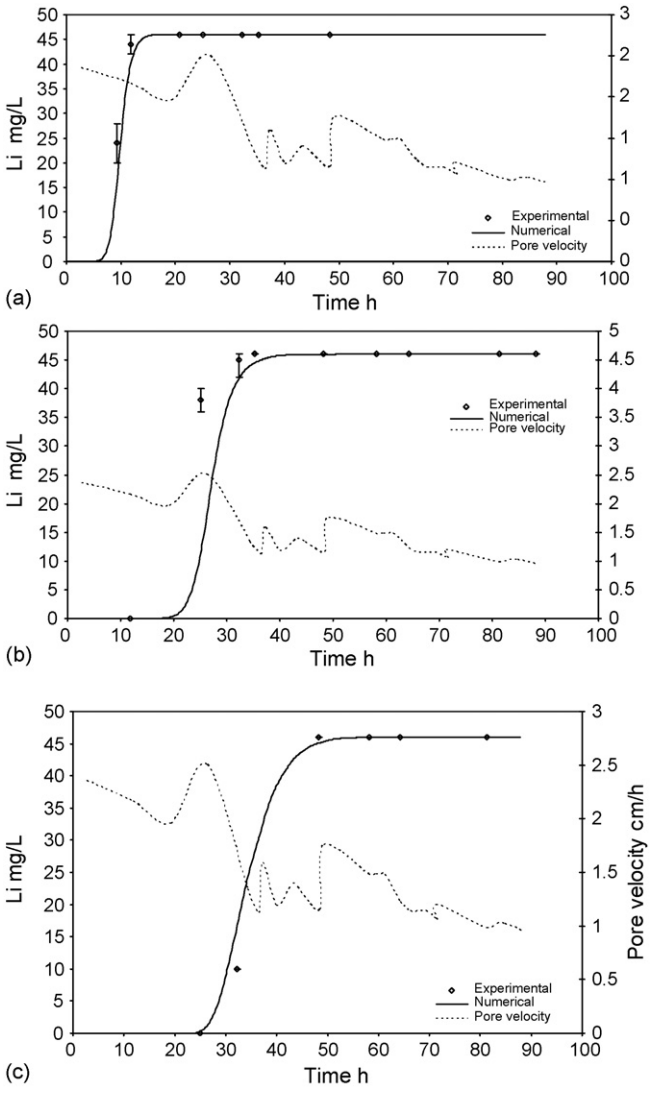


Fig. 14. Experimental and numerical lithium breakthrough curves of BB2; (pH 6.2–7.2, inlet Li concentration 46 mg/L, pore velocity 1.6 cm/h): (a) $x = 20$ cm, (b) $x = 49$ cm, (c) $x = 60$ cm.

Table 5
Input values for mathematical simulations of bio-barrier experiments

| S. No. | Parameter | Value |
|---|---|---|
| 1 | $\mu_{max}$ ($h^{-1}$) | 0.3 |
| 2 | $Y$ | 0.263 |
| 3 | $\eta$ | 0.3 |
| 4 | $\lambda$ for sand | 0.065 |
| 5 | $\lambda$ for Soil A | 0.1 |
| 6 | $K_s$ (mg/L) | 40.0 |
| 7 | $K_i$ (mg/L) | 3.049 |
| 8 | $K_d$ ($h^{-1}$) | 0.0 |

and 0.1805 mg/g in BB2. The column experiments also indicated some biotransformation on the upstream side of the bio-barrier. This may be due to the presence of small amount of biomass in the sand portion, which might have entered and accumulated through the feed or due to the movement of bacteria from the bio-barrier section of the column upstream into the sand sections. In the mathematical simulations, this concentration was assumed as 10 mg/L, which was almost negligible compared to the concentration of biomass in the barrier. As earlier, the dispersivity values for sand and barrier (Soil A) portions were estimated using the lithium breakthrough curves (0.01, 1.0). These values matched closely with the values estimated earlier for sand and Soil A. Values of $\lambda$ for sand and Soil A as determined from the earlier experiments were used here also.

Figs. 11–13 show the comparison between numerically simulated and experimental breakthrough curves for lithium, molasses, and Cr(VI) for BB1. It can be seen from Fig. 11a–c that the parameter estimation for dispersivity for BB1 is good,

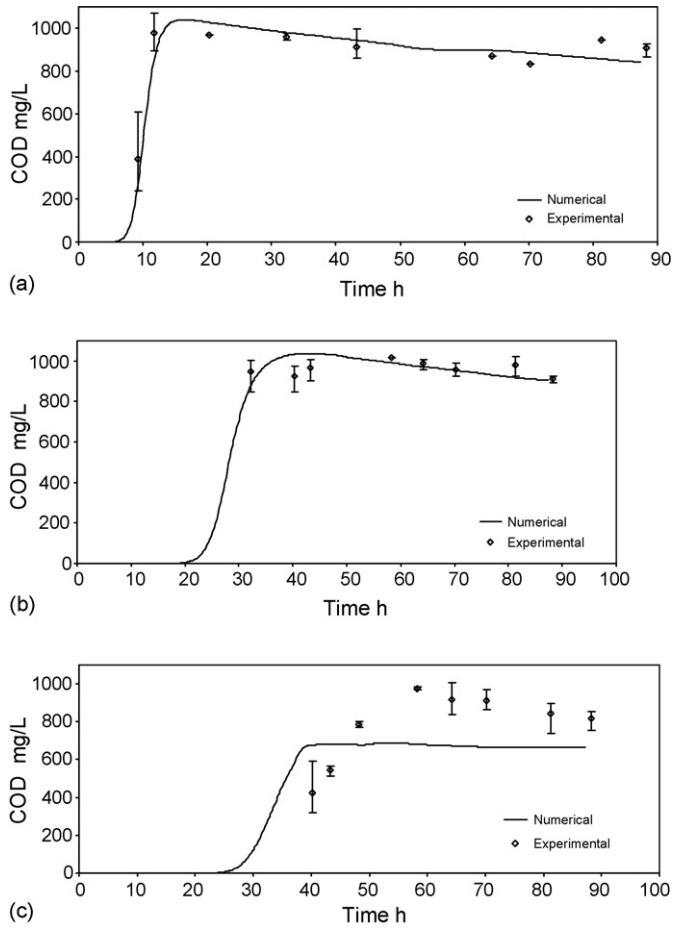


Fig. 15. Experimental and numerical substrate breakthrough curves of BB2; (pH 6.2–7.2, inlet COD concentration 1000 mg/L, pore velocity 1.6 cm/h): (a) $x = 20$ cm, (b) $x = 49$ cm, and (c) $x = 60$ cm.

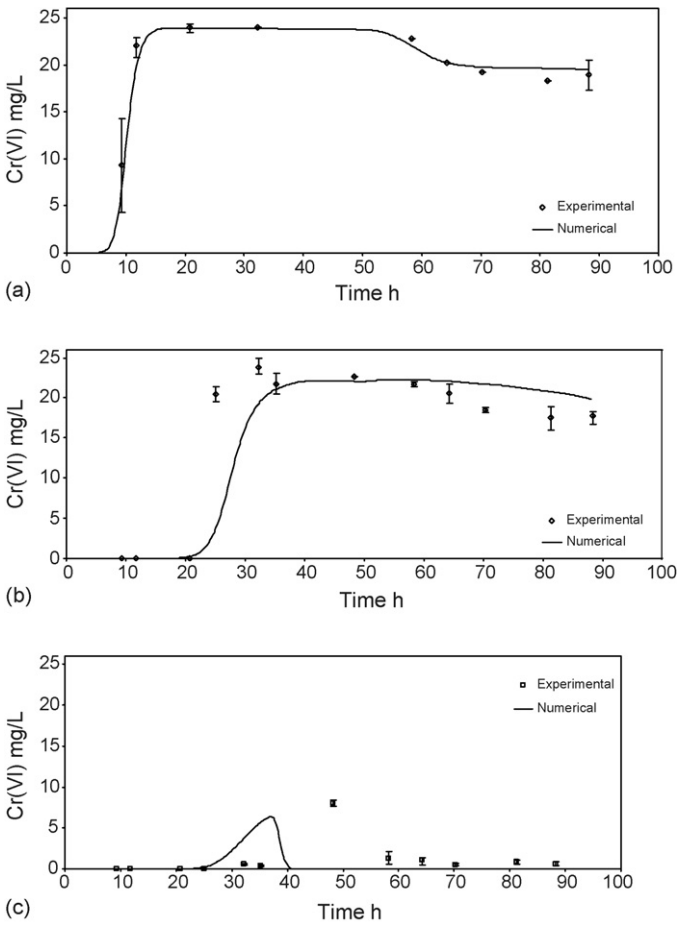


Fig. 16. Experimental and numerical Cr(VI) breakthrough curves of BB2; (pH 6.2–7.2, inlet Cr(VI) concentration 25 mg/L, pore velocity 1.6 cm/h): (a) $x = 20$ cm, (b) $x = 49$ cm, (c) $x = 60$ cm.

$E$ value varied from 0.77 to 0.96. However, the matching between the numerically simulated and experimental breakthrough curves was not good for molasses ($E$ value varied from 0.08 to 0.65). Similarly, the matching between the numerically simulated and experimental breakthrough curves for Cr(VI) was not as satisfactory ($E$ varied from −0.26 to +0.21). Although the proposed mathematical model simulated the overall trend of increasing biotransformation with distance and time, the quantification by the mathematical model was not satisfactory. Comparison between the numerical model and experimental results for BB2 are presented in Figs. 14–16, for lithium, molasses, and Cr(VI), respectively. It is evident from these figures that the matching between the numerical model and experimental results for Cr(VI) breakthrough was not as good, especially at the 60 cm port (downstream of barrier, $E = -0.46$). These results are in conformity with the earlier results that biotransformation affects the hydrogeology of the aquifer and increases the non-homogeneity. This affect was more significant in cases where the biomass concentration was high, as expected. Temporal variation of head loss from $x = 0$ to $x = 49$ cm (sand portion), and from $x = 49$ cm to $x = 60$ cm (bio-barrier) showed that there was a considerable increase in head loss (0–6 cm in 80 h) with respect to time in the bio-barrier portion, whereas the change in the head loss was almost negligible in the sand portion. This clearly indicates that the biotransformation process has an effect on the hydrogeology. As discussed earlier, present mathematical model does not consider the effect of biotransformation on hydrogeology.

Breakthrough curves for molasses at $x = 60$ cm clearly show that significant amount of molasses was unutilized even after the complete biotransformation of Cr(VI). This means more molasses was introduced, than what was truly required. In order to reduce the cost as well as associated contamination problems in field applications, optimization is required to determine the best combination of initial biomass concentration in the barrier, substrate concentration, and the bio-barrier thickness.

## 5. Conclusions

Bench scale transport and biotransformation studies showed that bio-barriers are an effective way of chromium containment in contaminated aquifers. Most significant parameters in the containment of Cr(VI) are pore water velocity and the initial biomass concentration. A simple mathematical model for the transport of Cr(VI) and molasses, coupled with adsorption and Monod's inhibition kinetics for immobile bacteria, was able to

simulate the experimental results satisfactorily when the clay content was less and the microbial activity was not very high. Clay content and increased heterogeneity in the system due to high bacterial activity altered the hydro-geological conditions. In such cases, there was disparity between the numerically simulated and experimental breakthrough curves for Cr(VI) and molasses.

## References


[1] C.W. Fetter, Contaminant Hydrogeology, Prentice Hall, Canada, 1993.

[2] R.J. Tobia, J.M. Camacho, P. Augustin, R.A. Griffiths, R.M. Frederick, Washing studies for PCP and creosote contaminated soil, J. Hazard. Mater. 38 (1994) 145–161.

[3] J.M. Chen, O.J. Hao, Microbial chromium(VI) reduction, Crit. Rev. Environ. Sci. Technol. 28 (3) (1998) 219–251.

[4] C. Liu, Y.A. Gorby, J.M. Zachara, J.K. Fredrickson, C.F. Brown, Reduction kinetics of Fe(III), Co(III), U(VI), Cr(VI) and Tc(VII) in cultures of dissimilatory metal-reducing bacteria, Biotechnol. Bioeng. 80 (6) (2002) 637–648.

[5] K. Rama Krishna, L. Philip, Bioremediation of Cr(VI) in contaminated soils, J. Hazard. Mater. 121 (2005) 109–117.

[6] J. Jeyasingh, L. Philip, Bioremediation of chromium contaminated soil: optimization of operating parameters under laboratory conditions, J. Hazard. Mater. 118 (2005) 113–120.

[7] J.L. Nyman, F. Caccavo Jr., A.B. Cunningham, R. Gerlach, Biogeochemical elimination of chromium(VI) from contaminated water, Bioremediation J. 6 (1) (2002) 39–55.

[8] C.H. Wang, C.P. Huang, P.F. Sanders, Transport of Cr(VI) in soils contaminated with chromite ore processing residue (COPR), Pract. Period. Hazard. Toxic Radioactive Waste Manage. 6 (2002) 6–13.

[9] H.M. Selim, M.C. Amacher, I.K. Iskandar, Modeling the Transport of Heavy Metals in Soils. USA Cold Regions Research and Engineering Laboratory, Hanover, NH, CRREL Monograph 90-2, 1990.

[10] M.C. Amacher, H.M. Sellim, Mathematical model to evaluate retention and transport of Cr(VI) in soil, Ecol. Model. 74 (1994) 205–230.

[11] H. Guha, J.E. Saiers, S. Brooks, P.M. Jardine, K. Jayachandran, Chromium transport, oxidation, and adsorption in manganese-coated sand, J. Contam. Hydrol. 49 (2001) 311–334.

[12] P.M. Jardine, S.F. Fendorf, M.A. Mayes, L. Larsen, S.C. Brooks, B. Bailey, Fate and transport of chromium in undisturbed heterogeneous soil, Environ. Sci. Technol. 33 (1999) 2939–2944.

[13] L. Philip, L. Iyengar, C. Venkobachar, Cr(VI) reduction by *Bacillus coagulans* isolated from contaminated soils, J. Environ. Eng. 124 (2) (1998) 1165–1170.

[14] H. Ohtake, E. Fujii, K. Toda, Bacterial reduction of hexavalent chromium: kinetic aspects of chromate reduction by *E. Cloacae* HO1, Biocatalysis 4 (1990) 227–235.

[15] P.T. Wong, J.T. Trevors, Chromium toxicity to algae and bacteria, in: J.O. Nriagu, E. Nieboer (Eds.), Chromium in the Natural and Human Environments, Wiley, New York, 1988, pp. 305–315.

[16] H. Guha, Bio-geochemical influence on transport of chromium in manganese sediments: experimental and modeling approaches, J. Contam. Hydrol. 70 (1–2) (2004) 1–36.

[17] T. Shashidhar, L. Philip, S. Murty Bhallamudi, Bench-scale column experiments to study the containment of Cr(VI) in confined aquifers by biotransformation, J. Hazard. Mater. B (13) (2005) 200–209.

[18] Compendium of Indian Standards on Soil Engineering. Part 1. Bureau of Indian Standards, India, 1989.

[19] G. Tchobanoglous, L.B. Franklin, H.D. Stensel, Metcalf and Eddy, Inc., Wastewater Engineering Treatment and Reuse, fourth ed., Tata McGraw-Hill Publishing Company Limited, New Delhi, 2003.

[20] American Public Health Association, American Water Works Association, and Water Pollution Control Federation, Standard Methods for the Examination of Water and Wastewater, 1995.

[21] D. Herbert, P.J. Phipps, J.E. Strange, Chemical analysis of microbial cells, in: J.R. Norris, D.W. Ribbons (Eds.), Methods in Microbiology, vol. 5B, Academic Press, New York, 1971.

[22] J. Ribesa, K. Keesmanb, H. Spanjers, Modelling anaerobic biomass growth kinetics with a substrate threshold concentration, Water Res. 38 (2004) 4502–4510.

[23] E.M. Murphy, T.R. Ginn, A. Chilakapati, C.T. Resch, J.L. Phillips, T.W. Wietsma, C.M. Spadoni, The influence of physical heterogeneity on microbial degradation and distribution in porous media, Water Resour. Res. 33 (1997) 1087–1103.

[24] P. Baveye, A.J. Valocchi, An evaluation of mathematical models of the transport of reacting solutes in saturated soils and aquifers, Water Resour. Res. 25 (1989) 1413–1421.

[25] G.T. Yeh, V.S. Tripathi, A model for simulating transport of reactive multispecies components: model development and demonstration, Water Resour. Res. 27 (12) (1991) 3075–3094.

[26] R. Srivastava, T.C. Jim Yeh, A three dimensional numerical model for water flow and transport of chemically reactive solute through porous media under variably saturated conditions, Adv. Water Resour. 15 (5) (1992) 275–287.

[27] A. Zysset, F. Stauffer, T. Dracos, Modeling of chemically reactive groundwater transport, Water Resour. Res. 33 (7) (1994) 2217–2228.

[28] D.R. Legates, G.J. McCabe Jr., Evaluating the use of goodness-of-fit measures in hydrologic and hydroclimatic model validation, Water Resour. Res. 35 (1) (1999) 233–241.

[29] J.M. Köhne, S. Köhne, J. Šimůnek, Multi-process herbicide transport in structured soil columns: experiments and model analysis, J. Contam. Hydrol. 85 (1–2) (2006) 1–32.